J. Chem. Sci. Vol. 129, No. 9, September 2017, pp. 1469–1481.
DOI 10.1007/s12039-017-1354-7

REGULAR ARTICLE

Synthesis, crystallographic characterization, DFT and TD-DFT studies of Oxyma-sulfonate esters

SAIED M SOLIMAN[a,b,*], HAZEM A GHABBOUR[c,d], SHERINE N KHATTAB[b], MOHAMMED R H SIDDIQUI[e] and AYMAN EL-FAHAM[b,e,*]

[a]Department of Chemistry, Rabigh College of Science and Art, King Abdulaziz University, P.O. Box 344, Rabigh 21911, Saudi Arabia
[b]Department of Chemistry, Faculty of Science, Alexandria University, P.O. Box 426, Ibrahimia, Alexandria 21321, Egypt
[c]Department of Pharmaceutical Chemistry, College of Pharmacy, King Saud University, Riyadh 11451, Saudi Arabia
[d]Department of Medicinal Chemistry, Faculty of Pharmacy, University of Mansoura, Mansoura 35516, Egypt
[e]Department of Chemistry, College of Science, King Saud University, P. O. Box 2455, Riyadh 11451, Saudi Arabia
E-mail: Saied1soliman@yahoo.com; aymanel_faham@hotmail.com

MS received 8 March 2017; revised 19 June 2017; accepted 7 July 2017; published online 29 August 2017

Abstract. Three oxyma sulfonate esters were prepared using dichloromethane-water (two-phase method) in the presence of sodium carbonate for scavenging HCl. The products were characterized by FT-IR, NMR (^{1}H and ^{13}C), UV-Vis spectra and elemental analysis. X-ray single crystal diffraction experiments proved the molecular structures of three esters. Their molecular structures were also calculated using DFT/B3LYP method. The optimized structures agreed well with the X-ray structures. Time-dependent density functional theory (TD-DFT) was used to assign the electronic absorption bands observed experimentally. Pyridine derivative showed two bands at shorter λ_{max} compared to the others, both experimentally and theoretically. The NMR chemical shifts were computed for protons and carbons using GIAO method, which correlated well with the experimental data. Natural charges, dipole moments and chemical reactivity of these molecules, as well as their non-linear optical activity, were computed and compared.

Keywords. Oxyma; sulfonate ester; X-ray crystallography; TD-DFT; NLO; NBO.

1. Introduction

Sulfonate esters are considered as important precursors for the synthesis of sulfonamides, which exhibit a wide range of biological activities.[1,2] The differences in their reactivity have been exploited in selective sulfonamide formation.[3] A comprehensive literature survey of the synthesis of sulfonamides revealed several synthetic strategies, which includes the methods for activation of the sulfonic acids to the corresponding 3-methylimidazoliumtriflates,[4] pentafluorophenolates,[5] sulfonyl benzotriazoles,[6] *p*-nitrophenolate esters,[7] and trichlorophenolates.[8] However, all the reported methods need either prolonged heating conditions or severe conditions such as using trifluoromethanesulfonic anhydride (TfO). Recently milder and more efficient method for the synthesis of sulfonamide by activating sulfonic acid group to the corresponding sulfonate ester of the ethyl 2-cyano-2-(hydroxyimino)acetate (Oxyma, **1**; Figure 1) was reported.[3]

Sulfonate ester of 1-hydroxybenzotriazole (HOBt **2**) derivatives has been synthesized and used for peptide coupling.[9,10] The reactivity of these sulfonate esters was affected by the presence of electron-withdrawing substituent in both the benzotriazole and the sulfonic acid moieties.[11–14] Later, 7-Aza-1-hydroxybenzotriazole (HOAt **3**)has been reported to be more efficient than HOBt **2** due to the electronic effect caused by the pyridine ring.[15,16] Because of the explosive report of HOBt**3**

*For correspondence

Electronic supplementary material: The online version of this article (doi:10.1007/s12039-017-1354-7) contains supplementary material, which is available to authorized users.

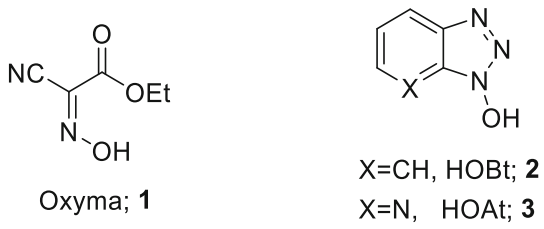

Figure 1. Structure of oxyma and benzotriazole derivatives.

and its derivatives,[17] ethyl 2-cyano-2-(hydroxyimino) acetate (Oxyma, **1**) has been used as a potential replacement for both HOBt and HOAt (Figure 1).[18,19]

Recently, *N*-alkyl-cyanoacetamido oximes **4-7**,[20–22] *N*-hydroxybenzimidoyl cyanide **8**, and *N*-hydroxypicolinimidoyl cyanide **9** (Figure 2), were reported and used for the preparation of sulfonate esters. The sulfonate esters **10–15** of the oximes shown in Figure 3 were evaluated for their anti-proliferation effect on the mouse fibroblast L929. The analysis showed that these compounds (**10–15**) have growth inhibition activity on L929 cells.[20]

Herein, we report a modified method for the synthesis of the sulfonate esters using dichloromethane-water (two-phase method) in the presence of sodium carbonate for the scavenging of the HCl. X-ray crystallography was used to determine the structures of the three prepared sulfonate esters. Time dependent density functional theory (TD-DFT) was used to assign their electronic spectra. The natural bond orbital analysis was performed to analyze the charge distributions and to study the different intramolecular charge transfer within the studied systems.

2. Experimental

2.1 *Materials and methods*

Melting points were determined with a Mel-Temp apparatus (Chemie GmbH, 82024 Taufkirchen, Germany). Nuclear magnetic resonance spectra (^{1}H NMR and ^{13}C NMR spectra) were recorded on a JEOL ECP-400 MHz spectrometer (JEOL Ltd., Tokyo, Japan) using $CDCl_3$ or DMSO-d_6 as solvent and reported in δ-units (Figures S1–S3, Supplementary data). Fourier transform infrared spectroscopy (FT-IR) spectra were recorded on Nicolet 6700 spectrometer (Thermo Scientific, Fishers, IN, USA) using KBr discs. Elemental analyses were performed on Perkin-Elmer 2400 elemental analyzer (Perkin Elmer Inc.,Waltham, MA USA). The solvents used were of HPLC reagent grade and all the chemicals were purchased from Sigma-Aldrich (Steinheim, Germany), Fluka (Steinheim, Germany). The reactions and the purity of the compounds were followed by TLC on silica gel-protected aluminum sheets (Type 60 GF254, Merck Millipore, Billerica, MA, USA) using UV lamp for spot visualization. The electronic spectra of the studied compounds were measured in different solvents such as acetonitrile, methanol and dichloromethane using UV-Vis spectroscopy (Perkin Elmer Lambda 35; Waltham, MA, USA).

2.2 *General method for the synthesis of oxyma derivative*

The two oximes **8** and **9** were synthesized according to the previously reported method[20] and used for the preparation of the sulfonate esters **11**, **14** and **16**.[20]

2.2a *General method for the synthesis of sulfonate esters*: The reported method[20] was modified as follows: To a solution of 5 mmol of oxime **8** (0.73g) or **9** (0.735g) and Na_2CO_3 (0.5g, 5 mmol) in 30 mL of dichloromethane (DCM)-water (1:1), 4-tosyl chloride **18a** (0.9g, 5 mmol) or 2-naphthalene sulfonyl chloride **18b** (1.135g, 5 mmol) in 15 mL of dichloromethane was added dropwise at 0°C. The reaction mixture was stirred at 0°C for 1 h and then at room temperature for 4 h. After completion of the reaction as monitored by TLC (ethylacetate-hexane; 4:6), 50 mL of CH_2Cl_2 was added, and the organic layer was collected and washed with water (20 mL) andsaturated aqueous NaCl (20 mL). It was finally dried over Na_2SO_4 anhydrous. After removal of the solvent under reduced pressure, the residue was recrystallized from CH_2Cl_2-hexane to give the sulfonate esters in their crystallized form.

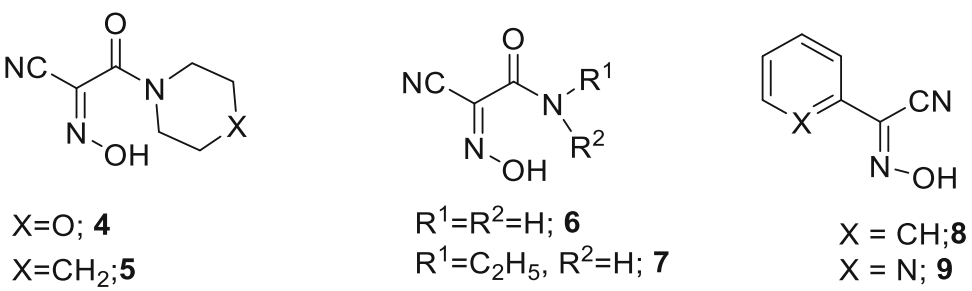

Figure 2. Structure of *N*-alkyl-cyanoacetamidooximes **4-7**, *N*-hydroxybenzimidoyl cyanide **8**, and *N*-hydroxypicolinimidoyl cyanide, **9**.

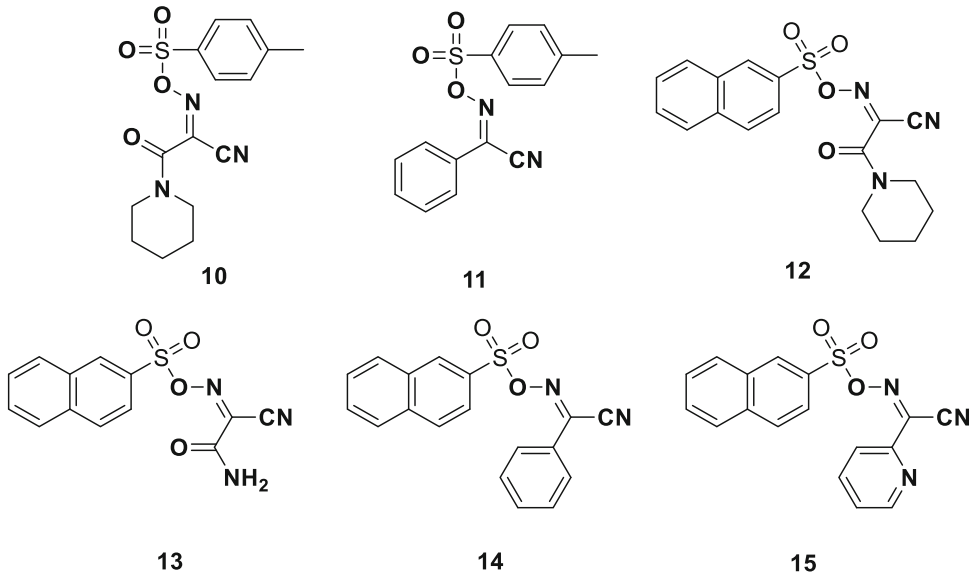

Figure 3. Structure of 4-tosyl esters **10, 11** and 2-naphthalenesulfonyl esters **12–15**.

2.2b *N-(tosyloxy)benzimidoyl cyanide* **(11)**: *The product was obtained as white crystals*, in 84% yield, M.p.: 112°C; [Lit[20] 85% yield, M.p.: 110–111°C]; IR (KBr, ν /cm^{-1}): 2242 (CN), 1393, 1187 (SO_2, sulfonate). ^{1}H NMR (400 MHz, $CDCl_3$) ppm: δ 2.45 (3H, s, CH_3), 7.39 (2H, d, Ar-H, J = 8.8 Hz), 7.46 (3H, t, Ar-H), 7.57 (1H, t, Ar-H, J = 7.3 Hz), 7.78 (2H, d, Ar-H, J = 8.0 Hz), 7.94 (1H, d, Ar-H, J = 8.0 Hz).^{13}C NMR (100 MHz, $CDCl_3$) ppm: δ 21.8, 107.7, 127.3, 127.5, 129.3, 129.4, 130.2, 131.2, 133.5, 139.4, 146.5. *Anal.* Calcd. for $C_{15}H_{12}N_2O_3S$: C, 59.99; *H*, 4.03; *N*, 9.33%. Found: C, 60.16; H, 4.25; N, 9.05%.

2.2c *N-(naphthalen-2-ylsulfonyloxy)benzimidoyl cyanide* **(14)**: The product was obtained as white crystals in 88%yield, M.p.: 134–135°C; [Lit[20] yield 86%, M.p.:133–134°C] IR (KBr, ν /cm^{-1}): 2234 (CN), 1390, 1186 (SO_2, sulfonate). ^{1}HNMR (400 MHz, $CDCl_3$) ppm: δ 7.44 (2H, t, Ar-H, J = 8.1 Hz), 7.54 (1H, t, Ar-H, J = 7.3 Hz), 7.65–7.78 (4H, m, Ar-H), 7.93–8.04 (4H, m, Ar-H), 8.65 (1H, s, Ar-H). ^{13}CNMR (100 MHz, $CDCl_3$) ppm: δ 107.6, 123.1, 127.1, 127.5, 128.1, 129.3, 129.6, 129.7, 130.0, 131.0, 131.6, 131.9, 133.4, 135.8, 139.5. *Anal.* Calcd. for $C_{18}H_{12}N_2O_3S$: C, 64.27; H, 3.60; N, 8.33%. Found: C, 64.11; H, 3.35; N, 8.05%.

2.2d *N-(tosyloxy)picolinimidoyl cyanide* **(16)**: The product was obtained as grey crystals, in 88% yield, M.p.: 129–130°C; IR (KBr, ν /cm^{-1}): 2247 (CN), 1394, 1173 (SO_2, sulfonate). ^{1}H NMR (400 MHz, $CDCl_3$) ppm: δ 2.46 (3H, s, CH_3), 7.39–7.47 (3H, m, Ar-H), 7.78–7.95 (4H, m, Ar-H), 8.72 (1H, d, Ar-H, J = 4.4 Hz) .^{13}CNMR (100 MHz, $CDCl_3$) ppm: δ 21.9, 107.4, 121.7, 126.9. 129.3, 130.2, 130.9, 137.3, 140.1, 146.8, 146.9, 150.4. *Anal.* Calcd. for $C_{14}H_{11}N_3O_3S$: C, 55.80; H, 3.68; N, 13.95%. Found: C, 55.96; H, 3.46; N, 14.09%.

2.3 *Crystal structures determination and refinement*

The compounds **11**, **14** and **16** were obtained as single crystals by slow evaporation from its solutions (dichloromethane-hexane; 2:1) to afford the pure compound at room temperature. Data were collected on a Bruker APEX-II D8 Venture area diffractometer, equipped with graphite monochromatic Mo $K\alpha$ radiation, λ = 0.71073 Å at 293 (2) K. Cell refinement and data reduction were carried out by Bruker SAINT. SHELXT[23,24] was used to solve the structure. The final refinement was carried out by full-matrix least-squares techniques with anisotropic thermal data for non-hydrogen atoms on F. CCDC 1456403, 1468844 and 1456418 contain the supplementary crystallographic data for this compounds **11**,**14** and **16**, respectively and can be obtained free of charge from the Cambridge Crystallographic Data Center via www.ccdc.cam.ac.uk/data_request/cif.

2.4 *Computational details*

The quantum chemical calculations were performed at the DFT/B3LYP level of theory and using the built in 6-31G(d,p) basis set as in Gaussian 03 software.[25] The input structures were taken from the crystallographic information files (CIFs) obtained from the X-ray single crystal measurements, which are reported here for the first time. The optimizations followed by frequency calculations at the optimized structures gave no imaginary frequency modes. In addition, the NMR chemical shifts and the UV-Vis electronic spectral bands were computed using the GIAO,[26,27] and Time Dependent-DFT (TD-DFT) methods,[28–30] respectively. The calculations were performed both in the gas phase and in presence of different solvents. The effects of solvent on the electronic spectra as well as the NMR chemical shifts were computed using solvent environment of the Polarizable Continuum Model (PCM). Relative chemical shifts are estimated by using corresponding

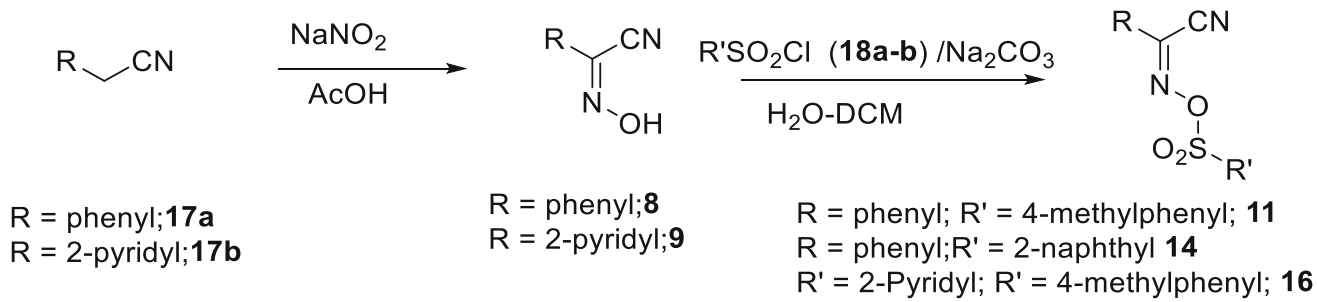

Scheme 1. Synthesis of oxyma sulfonate esters.

TMS shielding calculated in advance at the same theoretical level as the reference. GaussSum 2.2[31] was utilized to analyze the electronic spectra of the studied compounds. Moreover, the electronic properties affecting the nonlinear optical (NLO) properties of the studied systems were computed as obtained from the frequency calculations.

The natural bond orbital (NBO) calculations were performed using NBO 3.1 program as implemented in the Gaussian 03W package at the DFT/B3LYP level in order to understand various intramolecular charge transfer interactions between the filled orbitals of one subsystem and vacant orbitals of another subsystem, which is a measure of the intermolecular delocalization or hyper-conjugation.[32,33]

3. Results and Discussion

3.1 *Synthesis of oxyma sulfonate*

The two oxyma **8** and **9** were prepared from their aryl nitrile derivatives **17a, b** following the reported method,[19] and then reacted with the sulphonyl chloride derivatives **18a, b** using the modified two-phase method (DCM-H_2O) to afford the sulfonate esters **11**, **14** and **16** (Scheme 1) in excellent yields and purities as observed from their spectral data.

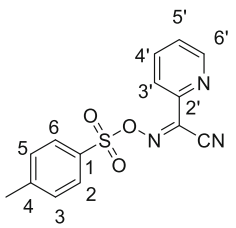

The ^{1}H NMR of *N*-(tosyloxy)picolinimidoyl cyanide **16** as a prototype showed a singlet peak at δ 2.46 related to CH_3group, multiplet peak at δ 7.39–7.47 corresponding to the three protons (H3,H5,H5'), multiplet peak at δ 7.78–7.95 corresponding to the four protons (H3',H4',H2 and H6), and doublet peak at δ 8.72 corresponding to the H6'. ^{13}C NMR of **16** showed carbon signal peaks at δ 21.9(CH_3), 107.4 (CN), 121.7(C3'), 126.9 (C5'), 129.3 (C2'), 130.2(C6), 130.9(C3,5), 137.3(C4'), 140.1(C4), 146.8(C1-SO_2), 146.9(C=N, Oxime), and 150.4(C2').

3.2 *X-ray crystallography*

Figure 4 presents the ORTEP diagrams of the compounds **11, 14** and **16**. Displacement ellipsoids are plotted at the 40% probability level for non-H atoms. The crystallographic data and refinement information are summarized in Table 1. The asymmetric units contain one independent molecule as shown in Figure 4. All the bond lengths and angles are within normal ranges.[34]

3.3 *DFT studies*

3.3a *Structure and electronic properties*: The calculated geometries using B3LYP method drawn using Chemcraft software[35] are shown in Figure 5. The overlay of the calculated and experimental X-ray structures indicated that the optimized molecular structures agreed well with the experimental results. Based on the calculated correlation coefficients (R^2) shown in Table S1 (Supplementary Information), the bond distances and angles obtained from the present calculations showed good correlations with the experimental data. The R^2 values for the bond distances and angles are in the range of 0.9886–0.9969 (Table S1, Supplementary Information).

The charge distribution has a direct relation to the polarity of the compound since the compounds have almost similar structure patterns. The natural bond orbital (NBO) calculations were used to predict the natural atomic charges (Q_{NAC}) at different atomic sites. The results of the natural atomic charges are given in Table 2. For all compounds, the three sulfonate O-atoms have the highest negative charge where the two free O-atoms are more negative than the third one. It is the least negative in case of the pyridine derivative. The Sulfur atom is electropositive in all the studied compounds where the Q_{NAC} is in the range 2.3910–2.3941e. The H-atoms are also electropositive. In contrast, all C-atoms

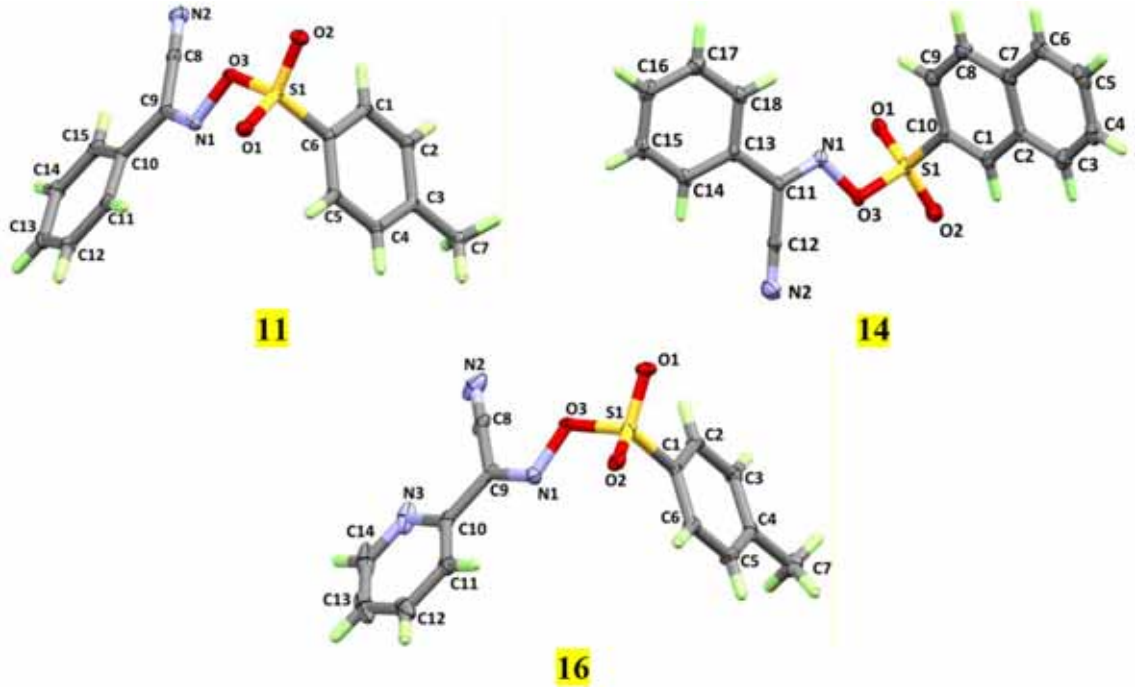

Figure 4. ORTEP diagrams of the **11**, **14** and **16**. Displacement ellipsoids are plotted at the 50% probability level for non-H atoms.

are electronegative except those attached to higher electronegative atoms such as nitrogen. The nitrile group (C ≡ N) nitrogen is richer in electrons than that for the C=N. In **16**, the most electronegative N-atom is the pyridine ring N-site. In this regard, a comparison between the calculated dipole moments of the studied compounds revealed that the dipole moment values were calculated to be 7.7231, 7.5512, and 8.7468 Debye for **11, 14** and **16**, respectively. It is clear that the presence of one more heteroatom (N) in the case of **16** leads to more polar structure than the others.

Map of the electron densities over the molecular electrostatic potential is a useful picture for predicting the electrophilic and nucleophilic region in the molecular systems. In these maps, the red regions are usually characterized by high electron densities and susceptible to be attacked by an electrophile. The dark blue regions are the most favored sites to be attacked by nucleophile as it is considered as electron poor regions. The maps of the molecular electrostatic potential (MEP) were drawn using GaussView software and shown in Figure 6. For all the studied system, the N and O-atom of the nitrile and sulfonate groups, respectively, are the most reactive to the attack of electrophile. It is clear that **16** has an electron-rich region around the N-atoms of the nitrile and pyridine rings. As a result, we could predict that this compound could act as good ligand in coordination chemistry than the others. The coordination of the metal ion as electrophile to these atomic sites of **16** is more favored over the others due to chelate effect. Dark blue regions around the S-atom of the sulfonate reveal the electron poor character of this atomic site in all compounds.

3.3b *Frontier molecular orbitals*: The frontier molecular orbitals HOMO and LUMO refer to the highest occupied and lowest unoccupied molecular orbitals, respectively. Their energies are important as they reflect the ability of the compound to give or take electrons (Table 3). The order of compounds according to HOMO energy is **14** > **11** > **16**. Hence, compound **14** is considered the most reactive compound towards electron donation. In contrast, **16** has the lowest energy LUMO orbital, and as a result is considered the best electron acceptor. In presence of solvent, all the HOMO levels are destabilized. The maximum destabilization occurred for **11**. On the other hand, all the LUMO levels are stabilized where the maximum stabilization occur for **16**. The difference in energy between HOMO and LUMO is the lowest amount of energy required for the electronic transition. Theoretically, the lowest transition energy is calculated to be 4.5294, 4.1451 and 4.6866 eV, for compounds **11**, **14** and **16**, respectively in the gas phase. In presence of acetonitrile as solvent, the electronic transitions become easier and require a lower amount of energy. Among all the studied compounds, **14** has the lowest transition energy either in the gas phase or solution, in agreement with the fact that the presence of more

Table 1. Crystal data for **11**, **14** and **16**.

	11	14	16
Crystal data			
Chemical formula	$C_{15}H_{12}N_2O_3S$	$C_{18}H_{12}N_2O_3S$	$C_{14}H_{11}N_3O_3S$
Mr	300.33	336.36	301.32
Crystal system, space group	Triclinic, *P*-1	Triclinic, *P*-1	Triclinic, *P*-1
Temperature (K)	100	100	100
a, *b*, *c* (Å)	5.4641 (3), 8.1232 (5), 15.8195 (9)	7.4962 (9), 7.4973 (9), 14.0427 (16)	5.2075 (6), 8.0975 (10), 16.426 (2)
α, β, γ(°)	100.840 (2), 98.332 (2), 97.180 (2)	87.459 (4), 77.948 (4), 80.483 (4)	90.911 (5), 98.825 (5), 97.860 (5)
V (Å^3)	673.93 (7)	761.16 (16)	677.52 (14)
Z	2	2	2
Radiation type	Mo *K* α	Mo *K* α	Mo *K* α
μ (mm^{-1})	0.25	0.23	0.25
Crystal size (mm)	0.48 × 0.27 × 0.14	0.36 × 0.21 × 0.15	0.37 × 0.19 × 0.06
Data collection			
Tmin, Tmax	0.889, 0.965	0.921, 0.966	0.913, 0.984
No. of measured, independent and observed [$I > 2\sigma(I)$] reflections	12941, 3096, 2639	9292, 3280, 2487	7960, 3082, 2076
R_{int}	0.045	0.050	0.082
Refinement			
R[$F^2 > 2\sigma(F^2)$], wR(F^2), S	0.038, 0.095, 1.04	0.046, 0.116, 1.03	0.059, 0.143, 1.01
No. of reflections	3096	3280	3082
No. of parameters	191	217	191
No. of restraints	0	0	0
$\Delta\rho_{max}$, $\Delta\rho_{min}$ (eÅ^{-3})	0.43, −0.42	0.44, −0.42	0.47, −0.44
CCDC No.	**1456403**	**1468844**	**1456418**

conjugated π-system in the compound lowers the energy gap between the HOMO and LUMO levels.

3.4 *UV-Vis electronic absorption spectra*

The experimentally measured UV-Vis electronic absorption spectra of the studied compounds in different solvents are shown in Figure S4 (Supplementary Information). All the studied compounds have two common transition bands. We noted a significant hyperchromic effect by changing the solvent from ACN to methanol to DCM to DMF. In contrast, changing the solvent showed very little effect on the λ_{max} values indicating that the solvent change exerts a very little effect on the energies of the molecular orbitals included in these transitions. From this point of view, we decided to perform TD-DFT calculations on one of these solvents to assign the obtained electronic transition bands. The maximum absorption wavelengths (λ_{max}) of the experimentally observed transition bands and the calculated λ_{max} values together with their oscillator strengths (f_{osc}) based on the TD-DFT calculations are given in Table 4.

The assignment of these electronic transition bands is given in the molecular orbital diagram shown in Figures 7 and S5–6 (Supplementary Information). For **14**, these two absorption bands are observed at 231 and 281 nm. The TD-DFT calculations predicted these bands at 235.6 nm ($f_{osc} = 0.029$) and 279.9 nm ($f_{osc} = 0.051$), respectively in the gas phase. In presence of acetonitrile as solvent, the λ_{max} of the longer wavelength band showed almost no variation but some decrease in its absorption intensity is noted. In contrast, hypsochromic shift and increase in the absorption intensity occurred for the shorter λ_{max} band with increasing solvent polarity from the gas phase to acetonitrile. The assignments of the electronic spectra shown in these figures revealed the higher energy transitions observed for compound **16** where the two bands were observed at shorter λ_{max} than

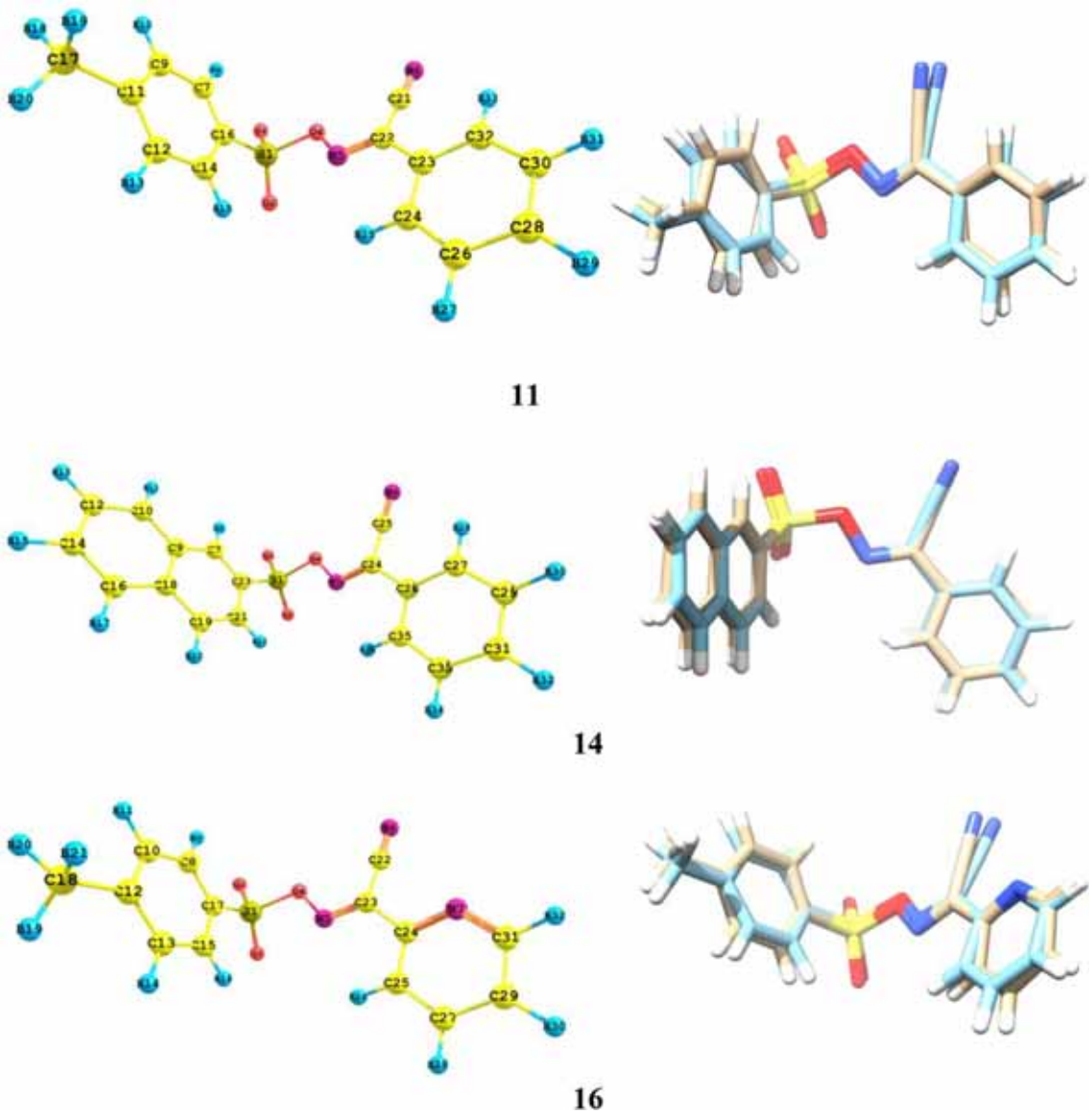

Figure 5. The optimized molecular structures of the studied compounds (left) and structure overlay between the calculated and X-ray single crystal structure (right).

the others, both experimentally and theoretically. These two bands were assigned to be mainly among molecular orbital with higher energy differences than those occurred in **14**.

3.5 *NMR spectra*

The nuclear magnetic resonance (NMR) chemical shifts were calculated using GIAO method in the gas phase and in the solution in order to match the results with those obtained experimentally. The calculated and experimental chemical shifts of the studied compounds are given in Table S2 (Supplementary Information). Correlations between the experimental and calculated ^{1}H- and ^{13}C-NMR chemical shifts were performed and the correlation coefficients are given in the same table. For compound **14**, the correlation is moderate in the gas phase (0.7712–0.7669) and generally improved (0.8114–0.8861) when solvent effects were considered. For the rest of the compounds, the correlation coefficients are high indicating the good correlations between the calculated and experimental data. It is worth noting that the presented calculation gave better correlations with the experimental data for protons than carbon. Usually, the opposite of this was common in literature.

3.5a *Nonlinear optical (NLO) properties*: Non-linear optical (NLO) effects occur when an intense beam of light such as laser interact nonlinearly with a material

Table 2. The calculated natural charges of the studied compounds.

11		14		16	
Atom	Q_{NAC}	Atom	Q_{NAC}	Atom	Q_{NAC}
S1	2.3937	S1	2.3941	S1	2.3910
O2	−0.8967	O2	−0.8950	O2	−0.8974
O3	−0.9002	O3	−0.9014	O3	−0.8965
O4	−0.5659	O4	−0.5658	O4	−0.5582
N5	−0.0935	N5	−0.0949	N5	−0.0905
N6	−0.2554	N6	−0.2549	N6	−0.2454
C7	−0.1994	C7	−0.1698	N7	−0.4358
H8	0.2727	H8	0.2713	C8	−0.1985
C9	−0.2288	C9	−0.0582	H9	0.2733
H10	0.2482	C10	−0.1994	C10	−0.2280
C11	0.0013	H11	0.2466	H11	0.2488
C12	−0.2302	C12	−0.2310	C12	0.0019
H13	0.2469	H13	0.2480	C13	−0.2304
C14	−0.1983	C14	−0.2200	H14	0.2469
H15	0.2721	H15	0.2470	C15	−0.1996
C16	−0.3573	C16	−0.2118	H16	0.2714
C17	−0.7051	H17	0.2434	C17	−0.3578
H18	0.2495	C18	−0.0429	C18	−0.7053
H19	0.2567	C19	−0.2003	H19	0.2482
H20	0.2483	H20	0.2477	H20	0.2501
C21	0.2378	C21	−0.2206	H21	0.2570
C22	0.1236	H22	0.2725	C22	0.2451
C23	−0.0885	C23	−0.3480	C23	0.1119
C24	−0.1985	C24	0.1246	C24	0.1678
H25	0.2603	C25	0.2378	C25	−0.2377
C26	−0.2320	C26	−0.0886	H26	0.2662
H27	0.2469	C27	−0.2079	C27	−0.2007
C28	−0.2173	H28	0.2558	H28	0.2519
H29	0.2455	C29	−0.2318	C29	−0.2632
C30	−0.2319	H30	0.2483	H30	0.2512
H31	0.2482	C31	−0.2170	C31	0.0268
C32	−0.2083	H32	0.2456	H32	0.2356
H33	0.2557	C33	−0.2319		
		H34	0.2470		
		C35	−0.1982		
		H36	0.2599		

to produce new fields, altered in its propagation characteristics like frequency or amplitude, compared to the incident fields.[36] NLO is a hot topic in chemistry and physics researches and it has many applications related to optical and electronic devices.[37–40] Organic systems having donor–acceptor π-conjugation are of interest in the field of nonlinear optical (NLO) properties. The nature of substituent and steric hindrance affects the degree of π-conjugation of the substances and hence its hyperpolarizability will be affected. As a result, the NLO of compound could be improved by the proper selection of substituent.[41]

Quantum chemical calculations can play an important role in the understanding of the structure–property relationship, which could be assisted in designing novel NLO materials. The components of polarizability (α) and hyperpolarizability (β) were used to calculate the total polarizability (α_{tot}) and hyperpolarizability (β_{tot}) using equations 1 and 2, respectively.

$$\alpha_{tot} = \frac{1}{3}\left(\alpha_{xx} + \alpha_{yy} + \alpha_{zz}\right) \quad (1)$$

$$\beta_{tot} = \left(\beta_{xxx} + \beta_{xyy} + \beta_{xzz}\right)^2 + \left(\beta_{yyy} + \beta_{yxx} + \beta_{yzz}\right)^2 + \left(\beta_{zzz} + \beta_{zxx} + \beta_{zyy}\right)^2 \quad (2)$$

The high values of polarizability (α) and the first hyperpolarizability (β) of the investigated molecules clearly reveal that they have nonlinear optical (NLO) behavior (Table 5). In comparison to urea (α_{tot} = 25.8793 A.U and β_{tot} = 43.1140 A.U), compounds **14**, **16** and **11** have α_{tot} values higher by 9.05, 7.44 and 7.63 times and β_{tot} values higher by 7.71, 2.66 and 5.83 times. The values of the total polarizability (α_{tot}) and hyper-polarizability (β_{tot}) shown in Table 5 indicated that **14** could be the best candidate for nonlinear optical applications as it has the highest α_{tot} and β_{tot} values compared to the others. The higher conjugation occurred in **14** due to the presence of naphthyl group could be the reason for such NLO enhancement.

3.5b *Second order perturbation energy analyses*: The analysis of the interaction energies between the filled natural bond orbitals (NBOs) and the empty ones shed light on the ease of electron delocalization among electron pairs in the studied systems. The interaction energies deduced from the NBO analyses were shown in Table S3 (Supplementary Information). The most important interactions occurred in the studied systems are π → π*, n → π* and n → σ* intramolecular charge transfer (ICT). Because all the studied molecules have conjugated π-system, so many π → π* ICT interactions were occurred. For **14**, the strongest π → π* ICT interaction has 20.40 kcal/mol for the BD(2)C33-C35 → BD*(2)C29-C31 charge transfer which is related to the phenyl ring π-system. Another ICT also have high stabilization energy (20.08 kcal/mol) takes place between one of the phenyl ring π-system as the donor (BD(2)C26-C27) and the BD*(2)N5-C24 as acceptor. In the case of **16**, the highest energy π → π* ICT interaction (28.14 kcal/mol) occurred among the pyridine ring π-bonds (BD(2)C25-C27 → BD*(2)N7-C24) while the second highest one (26.47 kcal/mol) is BD(2)C12-C13 → BD*(2)C15-C17 for the p-tolyl group. The latter occurred in **11** with almost the same ICT interaction energy (26.81 kcal/mol). For all compounds, there is only one significant n → π* ICT delocalization occurred from the second lone pair of O4 (LP(2)O4) to the π*-empty NBO of the adjacent N5=C

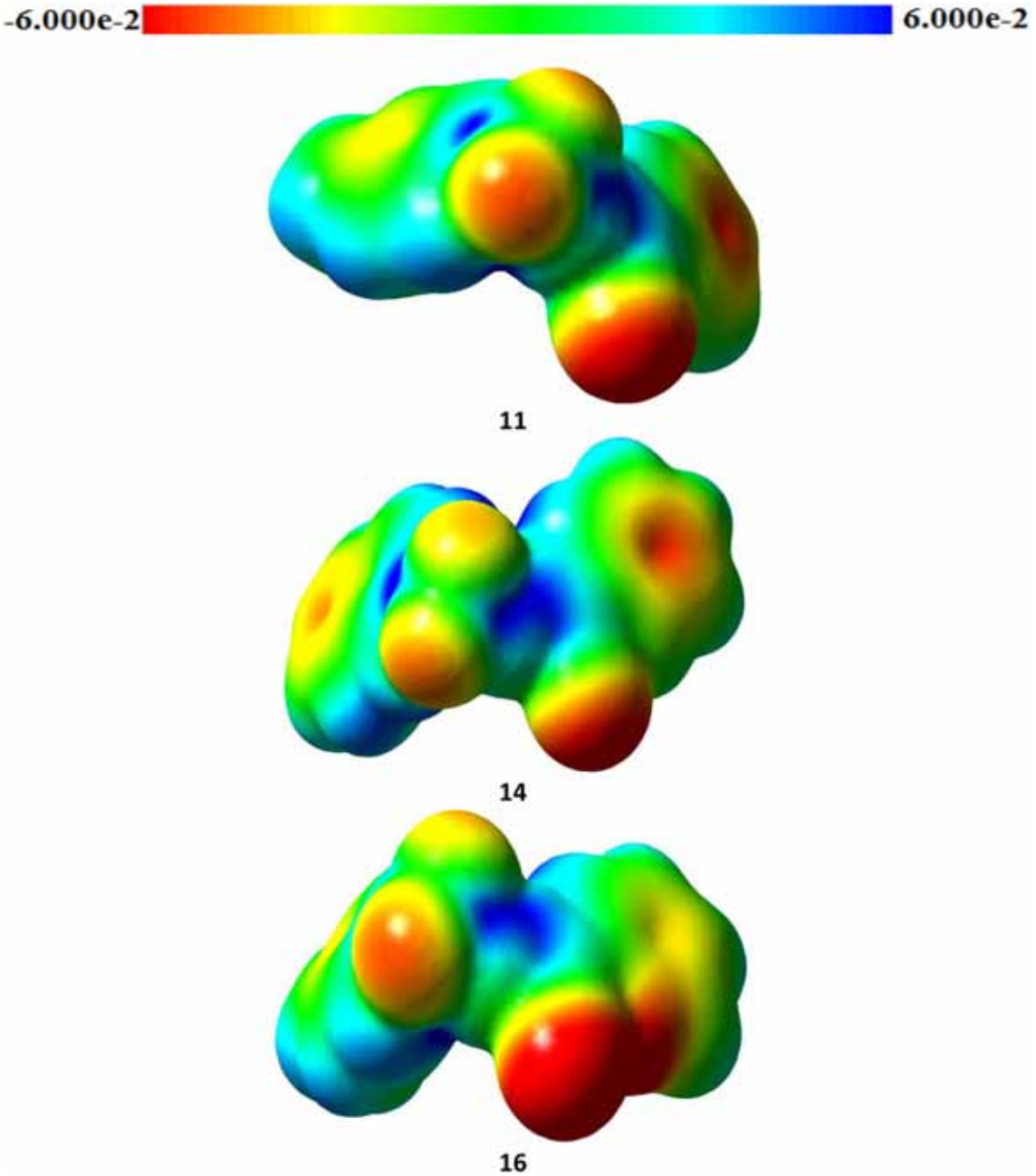

Figure 6. MEP maps of the studied compounds.

Table 3. The energies of the frontier molecular orbitals in the gas phase and in presence of acetonitrile as solvent.

	11		**14**		**16**	
	gas	ACN	gas	ACN	gas	ACN
HOMO	−6.9411	−6.8908	−6.5683	−6.3275	−7.1950	−7.1441
LUMO	−2.4118	−2.5154	−2.4232	−2.5258	−2.5084	−2.6384
Gap	4.5294	4.3754	4.1451	3.8017	4.6867	4.5057

Table 4. The calculated and experimental λ_{max} (nm) and their oscillator strengths.

(λ_{max})exp.	(λ_{max})calc	f_{osc}	Assignment
11			
227	229.6	0.344	H-5 → L (15%), H-1 → L+1 (61%)
282	258.7	0.071	H-4 → L (79%), H → L+2 (13%)
14			
231	233.8	0.919	H-2 → L+1 (27%), H-1 → L+2 (13%), H → L+2 (28%)
281	279.4	0.013	H-2 → L+1 (36%), H-1 → L+1 (15%), H → L+2 (41%)
16			
219	223.7	0.152	H-5 → L (36%), H-1 → L+1 (17%), H → L+2 (11%)
277	258.7	0.071	H-4 → L (79%), H → L+2 (13%)

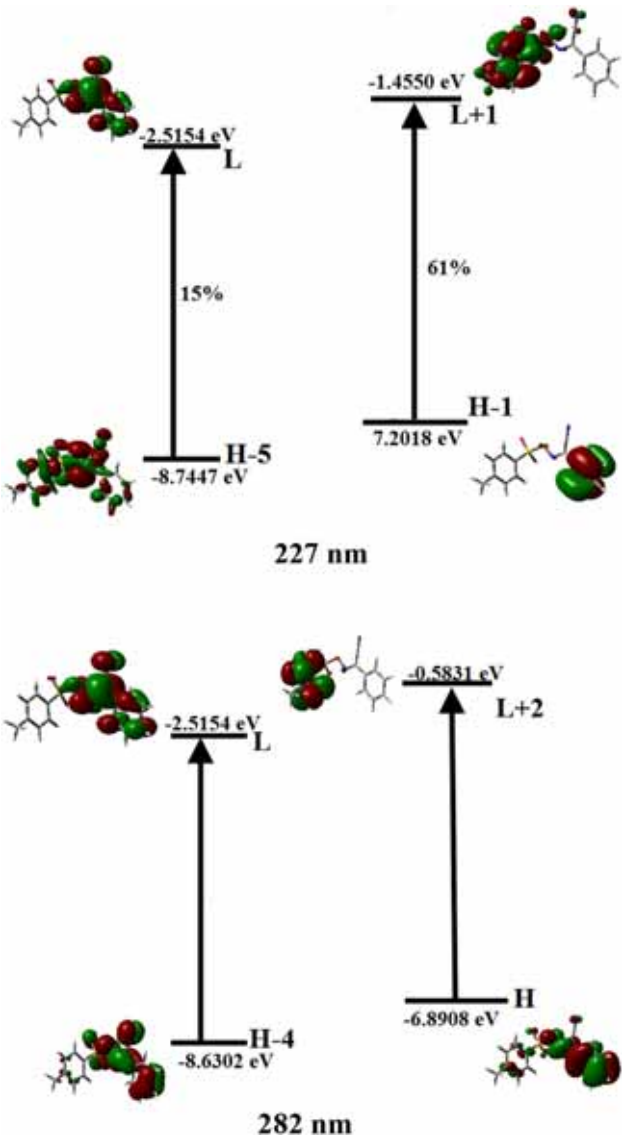

Figure 7. The origin of the most important spectral bands of **11**.

bond. The stabilization energies of these ICT interactions are 14.94, 18.43 and 15.62 kcal/mol for **11**, **14** and **16**, respectively. It is the maximum for **14**. In the two compounds having the p-tolyl group, this ICT interaction has almost the same strength. Two factors could lead to such variations: (1) the O4 atom has more deviation by 1° from the C=N5 bond in **11** and **16** compared to **14** which will slightly weaken LP(2)O4 → C = N; (2) the electronic factor where the naphthyl ring conjugated π-system could be a better electron donor to the sulphonate moiety than the p-tolyl group, this will make the O4-atom more e-rich and more ICT to the neighboring C=N bond will take place for **14** than the others. All the studied compounds have common features of n → σ* ICT interactions, all have 10 of these interactions except **16** has one more n → σ* ICT from LP(1)N7 → BD*(1)C24-C25 (10.28 kcal/mol) due to the replacement of the phenyl by pyridyl one. The highest of these interactions occurred from LP(3)O2 and LP(3)O3 filled NBOs to the empty σ* NBOs of the S1-O4 bond. These interactions stabilized the system upto 38.96, 38.21 and 38.16 kcal/mol for **14**, **16** and **11**, respectively.

3.5c *Reactivity descriptors*: Several reactivity descriptors such as ionization potential (I), electron affinity (A), chemical potential (μ), hardness (η) as well as electrophilicity index (ω) were proposed for understanding various aspects of reactivity associated with chemical reactions.[42–47] The definition of these parameters is given by Equations 1–5.

These chemical reactivity descriptors could be used for describing the different pharmacological and biological reactivity of compounds. Based on the molecular orbital calculations of the synthesized compounds, these reactivity descriptors are summarized and listed in Table 6. The results showed the order of the studied molecules according to chemical hardness is **16** > **11** > **14**. Compound **16** has the highest chemical hardness as it has one more electronegative atom in its structure. Moreover, all compounds have negative chemical potential so are considered stable compounds. It is well-known that

Table 5. The polarizability and hyperpolarizability components and their total values (A.U) of the studied compounds.

Parameter	11	14	16		11	14	16
α_{xx}	233.6056	285.5122	225.5522	β_{xxx}	119.5136	94.6122	−81.4442
α_{xy}	−15.2611	−3.9882	−13.3882	β_{xxy}	−166.5150	233.0252	−26.0682
α_{yy}	197.1262	222.3290	190.7274	β_{xyy}	47.1599	−62.4914	−38.3951
α_{xz}	3.6825	−25.3824	5.2904	β_{yyy}	−11.1243	97.9542	−55.7361
α_{yz}	−26.5293	27.5889	−23.8767	β_{xxz}	143.3713	116.2308	85.6555
α_{zz}	161.8942	194.8585	161.1696	β_{xyz}	−106.4500	−125.3100	−93.1212
				β_{yyz}	−41.5483	10.6334	−58.7575
				β_{xzz}	0.6574	−1.9668	13.2321
				β_{yzz}	35.2847	−27.8183	47.2213
				β_{zzz}	19.9696	6.4433	−3.4542
α_{tot}	197.5420	234.2332	192.4831	**βtot**	251.1929	332.5459	114.5019

Table 6. The quantum chemical reactivity parameters of compounds **12**, **14** and **16**.

Parameter	11	14	16
$I = -E_{HOMO}$	6.9411	6.5683	7.1950
$A = -E_{LUMO}$	2.4118	2.4232	2.5084
$\eta = (I - A)/2$	2.2647	2.0726	2.3433
$\mu = -(I + A)/2$	−4.6764	−4.4958	−4.8517
$\omega = \mu^2/2\eta$	4.8283	4.8760	5.0225

the flow of electrons could take place from the molecule with the highest chemical potential. From this point of view, the ability of the studied compounds to electron flow from it will be the highest for **14**. Moreover, the electrophilicity index of the studied compounds is in the order **16** > **14** > **11**. As a result, **16** has the highest electrophilicity index so it has higher electrophilic behavior compared to the others,[48] in agreement with a large number of strong electronegative atoms in this compound compared to the others.

4. Conclusions

The modified two-phase method of synthesis (using dichloromethane and water) gave three oxyma sulfonate esters in high yields and purities compared to the one-phase method (dichloromethane) in the presence of organic base triethylamine. The modified method is considered as an eco-friendly method without any contamination of trimethylamine, which was used in the previously reported method. The molecular structures of the three studied compounds were calculated and found to be agreeing with the X-ray structures. DFT calculations showed that the order of compounds according to polarity is **16** > **11** > **14**. Analyses of the electronic spectra were made using the TD-DFT method and the molecular orbitals involved in these electronic transitions were discussed. NBO method was used to calculate the natural atomic charges and investigate the intramolecular charge transfer interactions occurred in the studied systems. Chemical reactivity studies showed that the most electrophilic compound is **16** and the order of the studied molecules according to chemical hardness is **16** > **11** > **14**. According to the total polarizability (α_{tot}) and hyperpolarizability (β_{tot}), **14** could be the best candidate for nonlinear optical applications.

Supplementary Information (SI)

NMR and UV-Vis absorption spectra, Tables S1–S3 and Figures S1–S7 are given as supplementary information. For details see www.ias.ac.in/chemsci.

Acknowledgements

The authors extend their appreciation to the Deanship of Scientific Research at King Saud University for funding this work through research Group No. (RGP-234, Saudi Arabia).

References

1. Hangan A C, Turza A, Lianastan R, Sevastre B, Pàll E, Cetean S and Oprean L T S 2016 Synthesis, crystal structure and characterization of new biologically active Cu(II) complexes with ligand derived from *N*-substituted sulfonamide *J. Chem. Sci.* **128** 815
2. Tan C, de Noronha R G, Devi N S, Jabbar A A, Kaluz S, Liu Y, Mooring S R, Nicolaou K C, Wang B and Van Meir E G 2011 Sulfonamides as a New Scaffold for Hypoxia Inducible Factor Pathway Inhibitors *Bioorg. Med. Chem. Lett.* **21** 5528
3. Wilden J D, Geldeard L, Lee C C, Judd D B and Caddick S 2007 Trichlorophenol (TCP) sulfonate esters: A selective alternative to pentafluorophenol (PFP) esters and

sulfonyl chlorides for the preparation of sulfonamides *Chem. Commun.* 1074
4. O'Connell J F and Rapoport H 19921-Benzenesulfonyl- and 1-p-toluenesulfonyl-3-methylimidazolium triflates: Efficient reagents for the preparation of arylsulfonamides and arylsulfonates *J. Org. Chem.* **5** 7477
5. Caddick S, Wilden J D and Judd D B 2004 Direct Synthesis of Sulfonamides and Activated Sulfonate Esters from Sulfonic Acids *J. Am. Chem. Soc.* **126** 1024
6. Katritzky A R, Rodriguez-Garcia V and Nair S K 2004 A General and Efficient Synthesis of Sulfonylbenzotriazoles from *N*-Chlorobenzotriazole and Sulfinic Acid Salts *J. Org. Chem.* **69** 1849
7. Yan L, Bertarelli D C G, Hayallah A M, Meyer H, Klotz K N and Muller C E 2006 A New Synthesis of Sulfonamides by Aminolysis of *p* Receptor Antagonists *J. Med. Chem.* **49** 4384
8. Palakurthy N B, Nadimpally K C, Dev D, Rana S and Mandal B 2013 Sulfonamide Synthesis via Oxyma-*O*-sulfonates – Compatibility to Acid Sensitive Groups and Solid-Phase Peptide Synthesis *Eur. J. Org. Chem.* 2627
9. Kundu B, Shukla S and Shukla M 1994 Use of 1−β naphthalenesulfonyloxy benzotriazole as coupling reagent in solid phase peptide synthesis *Tetrahedron Lett*. **35** 9613
10. Khare S K, Singh G, Agarwal K C and Kundu B 1998 Use of 1 − β-Naphthalene sulfonyloxybenzotriazole as Coupling Reagent for Peptide Synthesis in the Presence of Fluorinated Alcohols as Cosolvent *Protein Pept. Lett*. **5** 171
11. Devedas B, Kundu B, Srivastava A and Mathur K B 1993 6-Nitro-l- β-Naphthalenesulfonyloxybenzotriazole: A Novel Coupling Reagent For Peptide Synthesis *Tetrahedron Lett*. **34** 6455
12. Carpino L A, El-Faham A and Albericio F 1994 Use of Onium Salt-Based Coupling Reagents in Peptide Synthesis *Tetrahedron Lett*. **35** 2279
13. Han Y, Albericio F and Barany G 1997 Occurrence and Minimization of Cysteine Racemization during Stepwise Solid-Phase Peptide Synthesis *J. Org. Chem.* **62** 4307
14. Carpino L A, Xia J, Zhang C and El-Faham A 2004 Organophosphorus and nitro-substituted sulfonate esters of 1-hydroxy-7-azabenzotriazole as highly efficient fast-acting peptide coupling reagents *J. Org. Chem.* **6** 962
15. Carpino L A 19931-Hydroxy-7-azabenzotriazole: An efficient peptide coupling additive *J. Am. Chem. Soc*. **115** 4397
16. Carpino L A, El-Faham A and Albericio F 1995 Efficiency in Peptide Coupling: 1-Hydroxy-7-azabenzotriazole vs 3,4-Dihydro-3-hydroxy-4-oxo-1,2,3-benzotriazine *J. Org. Chem*. **60** 3561
17. Wehrstedt K D, Wandrey P A and Heitkamp D 2005 Explosive properties of 1-hydroxybenzotriazole *J. Hazard. Mater*. **126** 1
18. Subirós-Funosas R, Prohens R, Barbas R, El-Faham A and Albericio F 2009 Oxyma: An efficient additive for peptide synthesis to replace benzotriazole-based HOBt and HOAt with a lower risk of explosion *Chem. Eur. J.* **15** 9394
19. Khattab Sh N 2010 Sulfonate Esters of 1-Hydroxypyridin-2(1H)-one and Ethyl 2-Cyano-2-(hydroxyimino)acetate (Oxyma) as Effective Peptide Coupling Reagents to Replace 1-Hydroxybenzotriazole and 1-Hydroxy-7-azabenzotriazole *Chem. Pharm. Bull*. **58** 501
20. El-Faham A, Elnakdy Y A, El Gazzar M S A, Abd El-Rahman M M and Khattab Sh N 2014 Synthesis, characterization and anti-proliferation activities of novel oximinosulfonate esters *Chem. Pharm. Bull.* **62** 373
21. Khattab Sh N, Subirós-Funosas R, El-Faham A and Albericio F 2012 Cyanoacetamide-based oxime carbonates: an efficient, simple alternative for the introduction of Fmoc with minimal dipeptide formation *Tetrahedron* **68** 3056
22. Khattab Sh N, Subirós-Funosas R, El-Faham A and Albericio F 2012 Screening of *N*Hydroxysuccinimide *Chemistry Open* **1** 147
23. Sheldrick G M Crystal structure refinement with *SHELXL* 2015 *Acta Crystallogr. C* **71** 3
24. Sheldrick G M, SHELXTL-PC (Version 5.1) 1997 *Siemens Analytical Instruments*, Inc., Madison, WI
25. (a) Frisch M J and *et al.,*2004 *Gaussian–03, Revision C.01, Gaussian, Inc*., Wallingford, CT; (b) GaussView, 2007 Version 4.1, Dennington R II, T Keith, J Millam, Semichem Inc., Shawnee Mission, KS
26. Ditchfield R 1972 Molecular orbital theory of magnetic shielding and magnetic susceptibility *J. Chem. Phys*. **56** 5688
27. Wolinski K, Hinton J F and Pulay P 1990 Efficient implementation of the gauge-independent atomic orbital method for NMR chemical shift calculations *J. Am. Chem. Soc*. **112** 8251
28. Petersilka M, Gossmann U J and Gross E K U 1996 Excitation Energies from Time-Dependent Density-Functional Theory *Phys. Rev. Lett.* **76** 1212
29. Bauernschmitt R and Ahlrichs R 1996 Treatment of electronic excitations within the adiabatic approximation of time dependent density functional theory *Chem. Phys. Lett.* **256** 454
30. Jamorski C, Casida M E and Salahub D R 1996 Dynamic polarizabilities and excitation spectra from a molecular implementation of time-dependent density-functional response theory: N_2 as a case study *J. Chem. Phys*. **104** 5134
31. O'Boyle N M, Tenderholt A L and Langner K M 2008 cclib: A library for package-independent computational chemistry algorithms *J. Comput. Chem*. **29** 839
32. Kisel V M, Kostyrko E O and Kovtunenko V A 2002 Synthesis and Biological Properties of Isoquinolines Spirofused with Carbocycles and Heterocycles at Position 4 *Chem. Heterocycl. Compd*. **38** 1295
33. Jarrahpour A, Ebtahimi E, De Clercq E, Sinou V, Latour C D, Bouktab L and Brunel J M 2011 Regio- and sterochemistry of the [2+2]-cycloaddition reaction between enones and alkenes. A DFT study *Tetrahedron* **67** 8699
34. Allen F H, Kennard O, Watson D G, Brammer L, Orpen A G and Taylor R 1987 Tables of bond lengths determined by *X*-ray and neutron diffraction. Part 1. Bond lengths in organic compounds *Part. J. Chem. Soc. Perkins Trans. II* 1
35. Zhurko G A and Zhurko D A 2005 *Chemcraft: Lite Version Build 08* (Freeware, Available online: http://www.chemcraftprog.com)

36. Sun Y X, Hao Q L, Wei W X, Yu Z X, Lu L D, Wang X and Wang Y S 2009 Experimental and density functional studies on 4-(3,4-dihydroxy benzylideneamino)antipyrine, and 4-(2,3,4-trihydroxybenzylideneamino)antipyrine *J. Mol. Str. Theochem*. **904** 74
37. Andraud C, Brotin T, Garcia C, Pelle F, Goldner P, Bigot B and Collet A 1994 Theoretical and experimental investigations of the nonlinear optical properties of vanillin, polyenovanillin, and bisvanillin derivatives *J. Am. Chem. Soc.* **116** 2094
38. Geskin V M, Lambert C and Bredas J L 2003 Origin of High Second- and Third-Order Nonlinear Optical Response in Ammonio/BoratoDiphenylpolyene Zwitterions: the Remarkable Role of Polarized Aromatic Groups *J. Am. Chem. Soc*. **125** 15651
39. Nakano M, Fujita H, Takahata M and Yamaguchi K 2002 Theoretical Study on Second Hyperpolarizabilities of Phenylacetylene Dendrimer: Toward an Understanding of Structure-Property Relation in NLO Responses of Fractal Antenna Dendrimers *J. Am. Chem. Soc*. **124** 9648
40. Sajan D, Joe H, Jayakumar V S and Zaleski J 2006 Structural and electronic contributions to hyperpolarizability in methyl p-hydroxy benzoate *J. Mol. Str.* **785** 43
41. Mahanalingam K, Nethaji M and Das P K 1996 Second harmonic generation in push-pull ethylenes: Influence of chirality and hydrogen bonding *J. Mol. Str.* **378** 177
42. Foresman J B, Frisch A E 1996 Exploring Chemistry with Electronic Structure Methods, second ed., Gaussian, Pittsburgh, PA.
43. Chang R 2001 *Chemistry* 7th edn. (New York: McGraw-Hill)
44. Kosar B and Albayrak C 2011 Spectroscopic investigations and quantum chemical computational study of (*E*)-4-methoxy-2-[(p-tolylimino)methyl]phenol *Spectrochim. Acta* **78** 160
45. Koopmans T A 1993 Über die Zuordnung von Wellenfunktionen und Eigenwertenzu den Einzelnen Elektronen Eines Atoms *Physica* 104
46. Parr R G and Yang W 1989 *Density-Functional Theory of Atoms and Molecules* (New York: Oxford University Press)
47. Parr R G, Von Szentpàly L and Liu S B 1999 Electrophilicity index *J. Am. Chem. Soc.* **121** 1922
48. Singh R N, Kumar A, Tiwari R K, Rawat P and Gupta V P 2013 A combined experimental and quantum chemical (DFT and AIM) study on molecular structure, spectroscopic properties, NBO and multiple interaction analysis in a novel ethyl 4-[2-(carbamoyl)hydrazinylidene]-3,5-dimethyl-1*H*-pyrrole-2-carboxylate and its dimer *J. Mol. Str*. **1035** 427